

# ZC3H7B-BCOR High-Grade Endometrial Stromal Sarcoma with a Muroid Grossly Feature: A Case Report and Literature Review

Wenxue Zhi , Xingzheng Zheng , Yulan Jin

Department of Pathology, Beijing Obstetrics and Gynecology Hospital, Capital Medical University, Beijing Maternal and Child Health Care Hospital, Beijing, 10006, People's Republic of China

Correspondence: Yulan Jin, Department of Pathology, Beijing Obstetrics and Gynecology Hospital, Capital Medical University, Beijing Maternal and Child Health Care Hospital, Beijing, 10006, People's Republic of China, Email 74000100@ccmu.edu.cn

**Abstract:** We report on a 50-year-old postmenopausal woman who presented with abnormal uterine bleeding and pelvic pain due to a uterine solid mass grew from the uterine fundus to the cervix and with so far undescribed obviously gelatinous grossly change, which was suspected of myxoid leiomyosarcoma in intraoperative diagnosis. Morphologically, the tumor cells displayed haphazard fascicles of uniform mild-to-moderate heteromorphic spindle cell component with significant and abundant myxoid stroma, forming signet ring cells and microcysts. Immunohistochemically, the tumour cells were diffusely positive for CD10 and cyclin D1 and negative for Desmin and SMA, but the expression of BCOR staining was not present. The FISH study showed a positive BCOR gene break probe, and the RNA sequencing revealed an identified reciprocal fusion gene ZC3H7B-BCOR. The case was finally diagnosed as ZC3H7B-BCOR high-grade endometrial stromal sarcoma. Tumor recurrence occurred rapidly on the pelvic peritoneal and vaginal 2 months after resection. In conclusion, these findings further support ZC3H7B-BCOR HGESS has a poor prognosis and molecular testing of uterine mesenchymal tumors with myxoid matrix and unusual grossly presentation is recommended to avoid misdiagnosis.

**Keywords:** ZC3H7B-BCOR, endometrial stromal sarcoma, postmenopausal woman

## Introduction

Endometrial stromal and related tumors are a rare and complex subset of mesenchymal uterine neoplasms. In the past decade, the classification of this rare group of tumors has changed significantly with the discovery of recurrent and mutually exclusive genomic alterations as next-generation sequencing analysis has been increasingly applied in clinical and research applications. Endometrial stromal and related tumours have been divided into four categories in the most recent classification by the World Health Organization (WHO, 2020): endometrial stromal nodule (NST), low-grade endometrial stromal sarcoma (LGESS), high-grade endometrial stromal sarcoma (HGESS) and undifferentiated uterine sarcoma (UUS),<sup>1</sup> and this distinction is predominantly guided by underlying genetic alterations. The most common HGESS are YWHAE-NUTM2 fusions HGESS containing t(10;17)(q22;p13), which consist of small, high-grade round cells arranged in lamellar and nested heterotypes with active mitotic figures. Recently, another newly identified group of ESS with a ZC3H7B-BCOR gene fusion was considered as a separate group of HGESS in addition to the known YWHAE-NUTM2 fusion, showing high malignant potential with more aggressive clinical behavior and different histological characteristics and immunohistochemical (IHC) expression.<sup>2</sup> However, due to its rarity, the clinicopathological features remain to be elucidated and awareness of this tumor should also be enhanced. Here, we report one case of ZC3H7B-BCOR fused HGESS with classic morphological characteristics and uncommon grossly finding.

A 50-year-old postmenopausal woman with abnormal uterine bleeding and pelvic pain, lasting one month. CT scan showed a large uterine mass, measuring 13.6 cm × 10.3 cm × 10 cm, with a high possibility of endometrial lesions and possible invasion of myometrium and upper cervix. Then, the patient underwent exploratory laparotomy. Intraoperative

findings were that the diameter of the posterior uterine wall mass was about 10 cm, with a gray-yellow cut surface. The mass infiltrates beyond the uterine serosal membrane. Scattered mass lesions can be seen on the surface of omentum, mesoappendix and mesentery of the small intestine. The patient had undergone a total abdominal hysterectomy with bilateral salpingo-oophorectomy and performed an intraoperative diagnosis. Grossly, the uterine solid mass grew from the uterine fundus to the cervix and up to 16 cm in size. It is located in the deep myometrium and partly penetrated the serosa with a tan-yellow and obviously gelatinous cut surface (Figure 1A). Frozen sections showed that the tumour was composed of fascicular spindle cells and had a destructive invasive pattern of the myometrium, which is associated with abundant myxoid stroma (Figure 1B). The cells have scant to moderate eosinophilic cytoplasm and mild-moderate nuclear atypia. Mitotic figures can easily be found in some areas in the section (Figure 1C), but necrosis was not seen. The intraoperative diagnosis was that it is a malignant mesenchymal tumour of the uterus with suspicious myxoid leiomyosarcoma (LMT). This patient had further resection of mass lesions on the surface of omentum, mesoappendix and mesentery of the small intestine. No residual mass was seen.

The permanent sections showed that most areas of the tumor cells with low cellularity have uniform nuclear features with mild-to-moderate nuclear atypia (Figure 2A), scant to moderate eosinophilic cytoplasm, inconspicuous nucleoli, and visible nuclear mitotic activity (5–6 mitoses/10 HPF of 0.55 mm in diameter). Some areas of the tumor cells with moderate cellularity were associated with moderate nuclear atypia with enlarged nuclei and increased nucleoplasm ratio and high mitotic count (16 mitoses/10 HPF of 0.55 mm in diameter) (Figure 2B). There was a significant and abundant myxoid stroma, with some cells appearing as cytoplasmic signet ring cell change (Figure 2C) or forming microcysts containing myxoid material or floating in mucin (Figure 2D). Thin-walled vessels were seen, with few arteriolar-type vessels and occasional thick-walled vessels. Lymphovascular invasion (LVSI) was not found. Most of the tumor cells showed a fascicular grown pattern, similar to leiomyoma-like tumor or LGESS. In some areas of the tumor, spindle cells were compacted and associated with collagenous plaques (Figure 2E). Rarely, benign endometrial glands were present on the tumor surface (Figure 2F).

Immunohistochemically, the tumor cells were diffusely positive for CD10 (Figure 3A) and cyclin D1 (Figure 3B), focal positive for PR and negative for ER, Desmin, SMA, h-Caldesmon, CD34, CD117, DOG1, ALK, pan-TRK and HMB45. The staining of p53 showed a wild-type expression pattern. Moreover, the tumor was negative for BCOR (Figure 3C).

Dual colour fluorescence in situ hybridisation (FISH) was performed using break-apart probes flanking *BCOR* (Xp11.4), *YWHAE*(17p13), *JAZF1*(7p15), *PHF1*(6p21) and *PLAG1*(8q12) (LBP Medicine Science and Technology, China). The FISH assay showed a positive BCOR gene break probe, indicating that a rearrangement of the BCOR gene had occurred (Figure 4), while FISH for *YWHAE*, *PHF1*, *JAZF1* and *PLAG1* rearrangements were all negative.

For RNA sequencing, genomic RNA was extracted from tumor Formalin-Fixed, Paraffin-Embedded (FFPE) samples using miRNeasy FFPE Kit. Ribosomal RNA was removed using RNase H followed by library preparation using KAPA Stranded RNA-seq Kit with RiboErase (HMR) (KAPA Biosystems). Library concentration and quality were determined by the Qubit 3.0 system (Invitrogen). Afterward, sequencing was performed by whole transcriptome RNASEQ detection

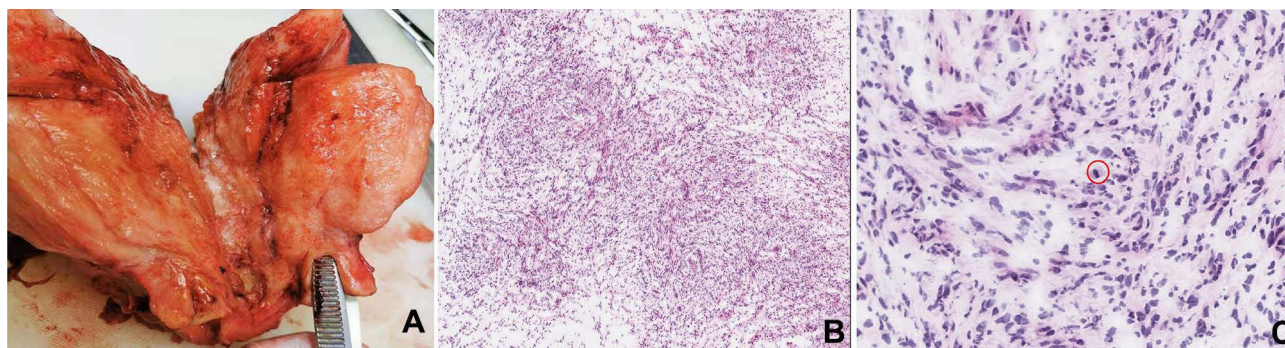


**Figure 1** Gross finding and frozen section microscopic presentation; (A) obviously gelatinous cut surface can be seen; (B) abundant myxoid matrix was seen in the background of the tumor (magnification 40x); (C) the spindle cells have mild-moderate cytologic atypia. Mitotic figures can easily be found (red circle) (magnification 200x).

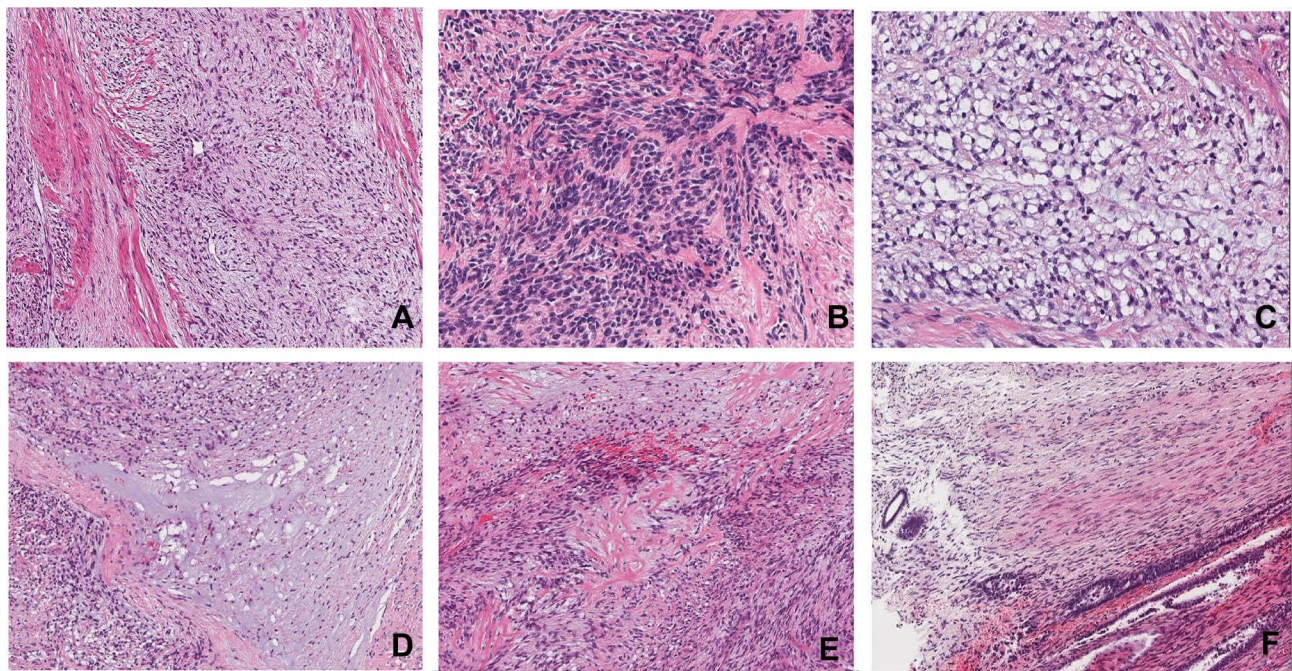


**Figure 2** Histological features of the tumor in postoperative paraffin sections; (A) spindle cells showing infiltrative growth within the myometrium with obvious myxoid matrix and thin-walled vessels (magnification 100x); (B) some tumor cells with moderate cellularity were associated of moderate cytological atypia with enlarged nuclei and high N/C ratio and high mitotic count (magnification 200x); (C) focally tumor was characterized by cytoplasmic vacuolation generated a signet-ring like appearance (magnification 200x); (D) abundant myxoid stroma formed multiple microcysts (magnification 100x); (E) focal collagenous plaques presenting (magnification 100x); (F) benign endometrial glands were present on the tumor surface (magnification 100x).

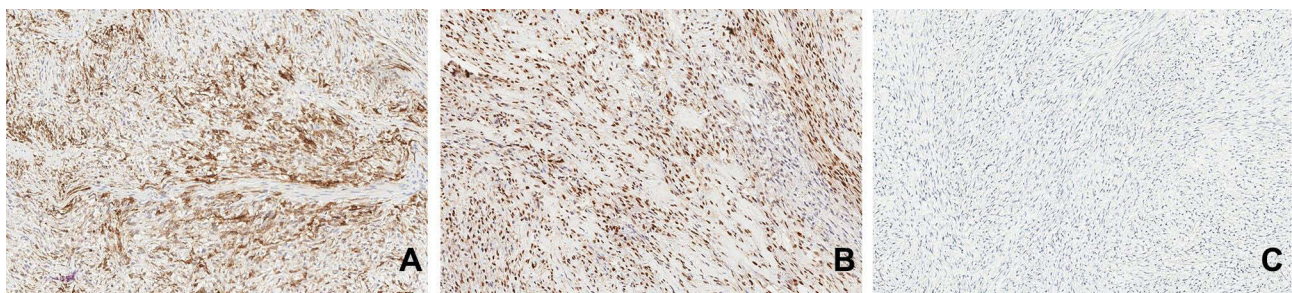


**Figure 3** Immunostaining results of ZC3H7B-BCOR HGESS; (A) CD10(+) (magnification 100x); (B) cyclinD1 (diffuse +) (magnification 100x); (C) BCOR(-) (magnification 100x).

(30M) on Illumina HiSeq 4000 according to the manufacturer's instrument. Genomic testing revealed a reciprocal fusion between BCOR exon 6 and ZC3H7B exon 11 (Figure 5).

Based on the histomorphological characteristics, IHC expression, FISH and RNA sequencing results, the case was finally diagnosed as ZC3H7B-BCOR HGESS. The tumor infiltrated the serosa with the presence of cervical deep stromal involvement. Tumor involvement in the omentum, mesoappendix and small intestine mesentery was seen. The patient with FIGO stage 3b received synchronous doxorubicin liposome chemotherapy and bevacizumab targeted therapy. CT imaging performed 2 months after resection showed an irregular mass on the pelvic peritoneal and upper right side of the vaginal stump with a maximum diameter of 3.7 cm, suggesting tumor recurrence. Six months after surgery, CT showed that the irregular mass increased to 5.4 cm and involved the right ureter. Multiple nodules in the abdominal cavity have increased in size compared to the previous one, considering the progression of tumor metastasis. The patient was treated with combined doxorubicin liposome chemotherapy with pablizumab immunotherapy for 4 cycles after synchronous doxorubicin liposome chemotherapy and bevacizumab targeted therapy for 6 cycles. The patient is currently alive 10 months after surgery but with severe renal insufficiency.

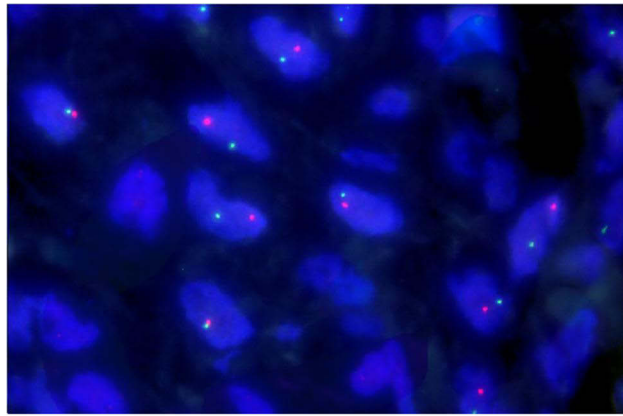


**Figure 4** FISH analysis confirmed gene rearrangements in BCOR showing split signals.

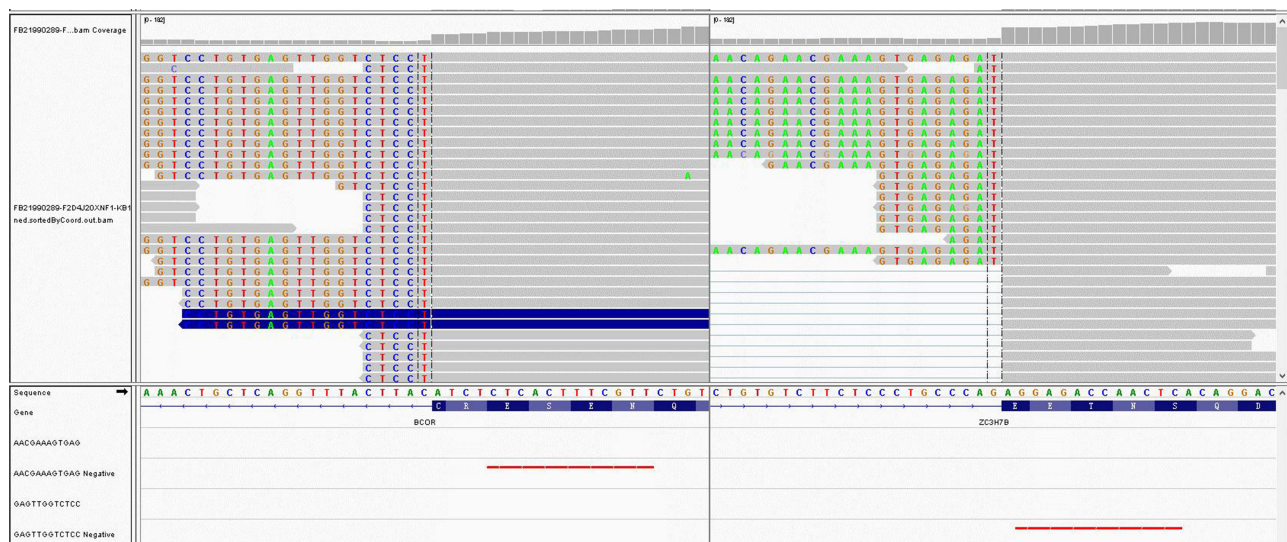


**Figure 5** RNA sequencing results show that the BCOR gene exon 6 is fused to the ZC3H7B gene exon 11.

## Discussion

There are three main independent molecular subgroups of HGESS in the 5th edition of WHO 2020, including YWHAENUTM2A/B HGESS, ZC3H7B-BCOR HGESS and HGESS with BCOR internal tandem duplication (ITD), with unique morphological features and IHC expression characteristics, respectively.<sup>1</sup> The specific molecular alteration of ZC3H7B-BCOR fusion occurring in ESS was first reported by Panagopoulos et al in 2013,<sup>3</sup> which reported two cases of ESS carrying the ZC3H7B-BCOR (t(X;22)(p11;q13)) fusion gene. Both cases consisted of spindle cells with mild cytological atypia and case 1 with low mitotic activity (0–1/10HPF) and positive for CD10, ER and PR. While case 2 had obvious vascular hyperplasia, a high mitotic count and was positive for CD10 but negative for ER and PR. Both patients had an advanced clinical stage and had distal ureteral and intestinal metastases, respectively. Subsequently, Hoang et al reported three cases of ESS with ZC3H7B-BCOR gene fusion sharing significant morphologic overlap with myxoid leiomyosarcoma of the uterus.<sup>4</sup> All cases displayed uniform spindle cells with abundant myxoid matrix and active mitotic activity. The tumor showed a “tongue-like” pattern of myometrium infiltration with involvement of endometrium and displayed aggressive clinical behavior. Lewis et al evaluated 17 cases of ZC3H7B-BCOR ESS in 2017, including five cases mentioned above, summarized the clinicopathological data, and proposed that ZC3H7B-BCOR fusion constituted a novel type of HGESS.<sup>2</sup> The patients were associated with unique histological features and worse prognosis compared to LGESS. Tumors usually involve the endometrium and infiltrate the myometrium in a tongue-like or push-type infiltration

pattern. Necrosis and LVSI were common. Morphologically, the tumor cells displayed haphazard fascicles of uniform spindle cells, which had intermediate-sized ovoid to spindle nuclei. The nucleus had uniform chromatin and generally inconspicuous nuclei. Cytoplasm ranged from scant to moderate and eosinophilic. Myxoid matrix was identified in most cases, with some forming lakes. Collagenous plaques and benign endometrial glands can be seen. The mitotic figures were brisk with a median of 14.5 mitotic figures/10 HPF. The vascular pattern was variable, and small arterioles were common and thick-walled vessels, which can be seen with occasional haemangiopericytoma-like patterns. IHC staining was often positive for CD10, cyclinD1 (diffuse in 86% of the tumors). Only 50% of cases were positive for BCOR. The expressions of ER and PR were variable, and smooth muscle markers were negative or weakly positive. Our current case encompassed almost all of the histological features and the immunoprofile mentioned above. The study also mentioned that the median age at diagnosis was 54 (range 28–71) years. Seven (41%), three (18%) and seven (41%) patients presented with FIGO stage 1, 2 and 3 disease, respectively. Eight of the 10 patients with follow-up data showed recurrence, revealing an aggressive clinical prognosis.<sup>2</sup> The case we reported was rapidly progressive, suggesting a poor clinical prognosis of this tumor consistent with the literature.

Subsequent reports of more cases enriched the histological and immunohistochemical expression characteristics of ZC3H7B-BCOR fused HGESS.<sup>5–8</sup> Other morphological features contained cytoplasmic signet ring cell changes, microcysts containing myxoid material, only focal myxoid matrix, a prominent haemangiopericytoma-like vascular pattern and small foci of osseous metaplasia. SATB2 can also be positively expressed. Positive expression of PAN-Trk in the cytoplasm or cell membrane may occur in some cases, but sequencing results showed no correlation with *Trk* gene rearrangement.<sup>9</sup>

However, morphological features and IHC profiles provide important diagnostic clues for ZC3H7B-BCOR HGESS, it still required FISH or molecular testing to confirm. BCOR is encoded by a BCL-6 interacting corepressor gene located on chromosome Xp11.4 that interacts with PCGF1 in a variant polycomb repressive complex (PRC1) to enhance transcriptional repression.<sup>10</sup> ZC3H7B participates in protein-nucleic acid interactions and thus may mediate its tumorigenic effect through abnormal epigenetic regulation. However, ZC3H7B-BCOR fusion is not unique to ESS. It has also been described in ossifying fibromyxoid tumor (OFT), which was a rare soft tissue neoplasm of uncertain differentiation and intermediate biologic potential.<sup>11</sup> OST also showed variably cellular spindle to round cells with myxoid to the collagenous stroma, but it most often affected the superficial and deep soft tissues of the extremities. The tumor was positive for S-100. Genomic alterations of BCOR via *ZC3H7B-BCOR* fusion or *BCOR* ITD in HGESS can be identified by IHC staining,<sup>12</sup> using the BCOR monoclonal antibody C-10. The BCOR monoclonal antibody detects *BCOR* exons 1, 2, 3 and some of the epitopes encoded by exon 4. Unfortunately, the positive expression of BCOR in *ZC3H7B-BCOR* HGESS was only about 50%. Someone assessed whether the differential expression of BCOR was associated with different breakpoints in the *BCOR* fusion transcripts, but no correlation was found.<sup>7</sup> Currently, there are four reported cases of *ZC3H7B* exon 10 -*BCOR* exon 7 gene fusion, among which three cases are positive for BCOR expression,<sup>5,12</sup> while one case is negative.<sup>7</sup> Other tumors with *ZC3H7B* exon 6-*BCOR* exon 14 fusion and *BCOR* exon 7-*ZC3H7B* exon 11 fusion were also positive for BCOR expression.<sup>5</sup> BCOR was negative in HGESS with *BCOR* exon 6-*ZC3H7B* exon 11 fusion. Interestingly, the current case we reported was also negative for BCOR expression with *BCOR* exon 6 and *ZC3H7B* exon 11 fusion. Such a coincidence indicates that whether there was a correlation between BCOR expression and specific breaking point needs to be clarified by accumulating more data and details in more cases. BCOR is also expressed in most female genital tract adenocarcinomas,<sup>13</sup> making the differential diagnostic value of BCOR IHC in *ZC3H7B-BCOR* HGESS less than ideal.

*ZC3H7B-BCOR* HGESS needs to be identified from other entities in female genital tumors, which share significant morphologic and IHC overlap. All of the useful differential diagnostic key points are summarized in Table 1. *YWHAENUTM2* HGESS is usually associated with lamellar, nest, pseudopapillary, or pseudoglandular round cells, without fasciculate spindle cells or obvious mucoid matrix.<sup>14</sup> Diffuse cyclinD1 and BCOR staining were observed in both of them,<sup>15</sup> but the expression of CD10, ER and PR was usually absent in round cell components of *YWHAENUTM2A/B*-fused HGESS. Both BCOR ITD HGESS and *ZC3H7B-BCOR* HGESS showed mild-to-moderate atypia spindle cells in significant fibromyxoid stroma, but *BCOR* ITD HGESS showed high-grade round cell components with severe nuclear atypia and brisk mitotic activities.<sup>16,17</sup> In IHC profiles, the expression of CD10 was negative or focal positive in *BCOR*

**Table 1** Helpful Features for Differential Diagnosis of ZC3H7B-BCOR HGESS

	Morphological Features	IHC Profiles	Molecular Alterations
ZC3H7B-BCOR HGESS	Fasciculate spindle cells and mucoid matrix	cyclinD1(+); BCOR(50%+); CD10(+), ER and PR (variable)	ZC3H7B-BCOR fusion
YWHAE-NUTM2 HGESS	High-grade round cells and LGESS component	cyclinD1(+); BCOR(+); CD10, ER and PR(-)	YWHAE-NUTM2A/B fusion
BCOR ITD HGESS	High-grade round cells and spindle cells	cyclinD1(+); BCOR(+); CD10(-/focal); ER and PR(variable)	BCOR ITD
LGESS with fibromyxoid stroma	Low-grade spindle cells and fibromyxoid stroma	cyclinD1(-); BCOR(-); CD10(+); ER and PR(+)	JAZF1-SUZ12 fusion; PPH1-JAZF1 and PPH1-EPC1 fusion
Myxoid LMS	Spindle cells with cigar-like nucleus; mucinous stroma; large thick-walled vessels	Desmin, SMA and h-Caldesmon(+); CD10(-); ER and PR(+)	PLAG1 gene fusion
IMT	Mixture of epithelioid and spindle cells; inflammatory infiltration	Desmin, SMA and h-Caldesmon(+); CD10, ER and PR(variable); ALK(+)	ALK gene rearrangement

**Abbreviations:** HGESS, high-grade endometrial stromal sarcoma; LGESS, low-grade endometrial stromal sarcoma; BCOR ITD, BCOR internal tandem duplication; LMS, leiomyosarcoma; IMT; inflammatory myofibroblastic tumor.

ITD HGESS. ZC3H7B-BCOR HGESS also needs to be differentiated from LGESS with fibromyxoid stroma. LGESS cells were low-grade with mild cytologic atypia, no obvious nucleoli, and usually low mitotic index.<sup>18</sup> Although CD10 was expressed in both of them, ER and PR were positive and cyclinD1 was negative in most LGESS.<sup>15</sup> Furthermore, BCOR was exactly negative in LGESS, thus it was a valuable diagnostic marker for distinguishing HGESS from LGESS.<sup>19</sup> The most common molecular alterations in LGESS were JAZF1-SUZ12 gene fusion caused by t(7) and PPH1-JAZF1 and PPH1-EPC1 fusion involving PPH1 gene on chromosome 6.<sup>20</sup>

Myxoid leiomyosarcoma (LMS) is also one of the most important differential diagnosis of ZC3H7B-BCOR HGESS. It was reported that some ZC3H7B-BCOR HGESS cases were misdiagnosed as myxoid leiomyosarcoma without FISH or next-generation sequencing because of obvious histological overlap between them.<sup>4</sup> Myxoid stroma, thick-walled vessels and collagenous plaques, which were common in smooth muscle tumors, can also be observed in ZC3H7B-BCOR HGESS. However, tumor cells of myxoid LMS were more common with a cigar-like nucleus and destructive myometrial invasion.<sup>21</sup> Recent studies have shown that PLAG1 gene fusion exists in 25% of myxoid leiomyosarcomas, which can be detected by FISH or PLAG1 IHC staining, suggesting that PLAG1 may be a useful diagnostic marker for them.<sup>22</sup> Previously, some researchers suggested that gross features may also be helpful for differential diagnosis. Myxoid LMS was usually grossly gelatinous or myxoid, which was not present in ZC3H7B-BCOR HGESS.<sup>4</sup> However, our current case was characterized by a myxoid grossly feature, which led us to consider it as myxoid LMS in intraoperative diagnosis. We suggested that the myxoid grossly feature cannot completely rule out the diagnosis of ZC3H7B-BCOR HGESS.

Another uterus mesenchymal tumor with myxoid stroma that should be identified was an inflammatory myofibroblastic tumor (IMT). As a kind of really histologically rare tumor, IMT was purely fascicular or myxoid or showed the predominance of one or the other pattern, composed of a mixture of epithelioid and spindle cells with mild to severe nuclear atypia.<sup>23,24</sup> Inflammatory infiltration dominated by lymphocyte infiltration was seen in all IMT, and no LVSI was found. IMT cells were positive for desmin, SMA and h-Caldesmon, and variable for CD10, ER and PR. Specific positive expressions of ALK or ALK gene rearrangement detected by FISH were the most useful diagnostic clues.

In summary, ZC3H7B-BCOR HGESS is a rare and unique group of ESS, which should be distinguished from other uterine mesenchymal tumors with myxoid matrix. Our case report adds a previously undescribed myxoid grossly feature to ZC3H7B-BCOR HGESS. Histologically, the consistent fascicular arrangement in the myxoid stroma, mild-to-moderate heteromorphic spindle cells and specific immunoprofile of CD10 and cyclinD1 and/or BCOR are useful diagnostic clues for the tumor, which should be further confirmed by molecular detection. ZC3H7B-BCOR HGESS is

prone to recurrence and has a poor prognosis. More case reports and more complete clinicopathological data were expected to raise awareness to avoid misdiagnosis.

## Statement of Ethics

We confirm that written informed consent was provided by the patient to have the case details and accompanying images published. The study complies with hospital ethical standards and received institutional approval to publish the case details. The authors have no ethical conflicts to disclose.

## Acknowledgments

We are grateful to Nanjing Geneseeq Technology Inc. for the technical help in sequencing.

## Funding

The study was supported by Wu Jieping Medical Foundation (No. 320.6750.2021-21-12).

## Disclosure

The authors report no conflicts of interest in this work.

## References

1. *Female Genital Tumours: WHO Classification of Tumours*. 5th ed. Lyon, France: IARC Publications; 2020.
2. Lewis N, Soslow RA, Delair DF, et al. ZC3H7B-BCOR high-grade endometrial stromal sarcomas: a report of 17 cases of a newly defined entity. *Mod Pathol*. 2018;31:674–684. doi:10.1038/modpathol.2017.162
3. Panagopoulos I, Thorsen J, Gorunova L, et al. Fusion of the ZC3H7B and BCOR genes in endometrial stromal sarcomas carrying an X;22-translocation. *Genes Chromosomes Cancer*. 2013;52:610–618. doi:10.1002/gcc.22057
4. Hoang LN, Aneja A, Conlon N, et al. Novel high-grade endometrial stromal sarcoma: a morphologic mimicker of myxoid leiomyosarcoma. *Am J Surg Pathol*. 2017;41:12–24. doi:10.1097/PAS.0000000000000721
5. Ondic O, Bednářová B, Ptáková N, et al. ZC3H7B-BCOR high-grade endometrial stromal sarcoma may present as myxoid sarcoma with cytoplasmic signet ring cell change. *Virchows Arch*. 2020;476:615–619. doi:10.1007/s00428-020-02744-5
6. Lu B, Chen J, Shao Y, Shi H. Two cases of ZC3H7B-BCOR high grade endometrial stromal sarcoma with an extension on its morphological features. *Pathology*. 2020;52:708–712. doi:10.1016/j.pathol.2020.05.007
7. Mansor S, Kuick CH, Lim SL, et al. ZC3H7B-BCOR-rearranged endometrial stromal sarcomas: a distinct subset merits its own classification? *Int J Gynecol Pathol*. 2019;38:420–425. doi:10.1097/PGP.0000000000000523
8. Nagaputra JC, Goh RCH, Kuick CH, et al. ZC3H7B-BCOR high-grade endometrial stromal sarcoma with osseous metaplasia: unique feature in a recently defined entity. *Hum Pathol Case Rep*. 2019;15:54e8.
9. Solomon JP, Linkov I, Rosado A, et al. NTRK fusion detection across multiple assays and 33,997 cases: diagnostic implications and pitfalls. *Mod Pathol*. 2020;33:38–46. doi:10.1038/s41379-019-0324-7
10. Huynh KD, Fischle W, Verdin E, Bardwell VJ. BCoR, a novel corepressor involved in BCL-6 repression. *Genes Dev*. 2000;14:1810–1823. doi:10.1101/gad.14.14.1810
11. Linos K, Kerr DA, Baker M, et al. Superficial malignant ossifying fibromyxoid tumors harboring the rare and recently described ZC3H7B-BCOR and PHF1-TFE3 fusions. *J Cutan Pathol*. 2020;47:934–945. doi:10.1111/cup.13728
12. Chiang S, Lee CH, Stewart CJR, et al. BCOR is a robust diagnostic immunohistochemical marker of genetically diverse high-grade endometrial stromal sarcoma, including tumors exhibiting variant morphology. *Mod Pathol*. 2017;30:1251–1261. doi:10.1038/modpathol.2017.42
13. Muthukumarana V, Fix DJ, Stolnicu S, et al. BCOR expression in mullerian adenocarcinoma: a potential diagnostic pitfall. *Am J Surg Pathol*. 2020;44:765–770. doi:10.1097/PAS.0000000000001445
14. Sciallis AP, Bedroske PP, Schoolmeester JK, et al. High-grade endometrial stromal sarcomas: a clinicopathologic study of a group of tumors with heterogeneous morphologic and genetic features. *Am J Surg Pathol*. 2014;38:1161–1172. doi:10.1097/PAS.0000000000000256
15. Lee CH, Ali RH, Rouzbahman M, et al. Cyclin D1 as a diagnostic immunomarker for endometrial stromal sarcoma with YWHAEFAM22 rearrangement. *Am J Surg Pathol*. 2012;36:1562–1570. doi:10.1097/PAS.0b013e31825fa931
16. Mariño-Enriquez A, Lauria A, Przybyl J, et al. BCOR internal tandem duplication in high-grade uterine sarcomas. *Am J Surg Pathol*. 2018;42:335–341. doi:10.1097/PAS.0000000000000993
17. Bouchoucha Y, Tauziède-Espariat A, Gauthier A, et al. Intra- and extra-cranial BCOR-ITD tumours are separate entities within the BCOR-rearranged family. *J Pathol Clin Res*. 2022;8:217–232. doi:10.1002/cjp2.255
18. Chiang S, Oliva E. Recent developments in uterine mesenchymal neoplasms. *Histopathology*. 2013;62(1):124–137. doi:10.1111/his.12048.
19. Alkanat NE, Uner A, Usbutun A. High-grade endometrial stromal sarcoma: morphologic and clinical features, the role of immunohistochemistry and fluorescence in situ hybridization in diagnosis. *Int J Surg Pathol*. 2022;4:10668969221098087.
20. Micci F, Heim S, Panagopoulos I. Molecular pathogenesis and prognostication of “low-grade” and “high-grade” endometrial stromal sarcoma. *Genes Chromosomes Cancer*. 2021;60:160–167. doi:10.1002/gcc.22907
21. Parra-Herran C, Schoolmeester JK, Yuan L, et al. Myxoid leiomyosarcoma of the uterus: a clinicopathologic analysis of 30 cases and review of the literature with reappraisal of its distinction from other uterine myxoid mesenchymal neoplasms. *Am J Surg Pathol*. 2016;40:285–301. doi:10.1097/PAS.0000000000000593

22. Arias-Stella JA, Benayed R, Oliva E, et al. Novel PLAG1 gene rearrangement distinguishes a subset of uterine myxoid leiomyosarcoma from other uterine myxoid mesenchymal tumors. *Am J Surg Pathol*. 2019;43:382–388. doi:10.1097/PAS.0000000000001196
23. Bennett JA, Nardi V, Rouzbahman M, et al. Inflammatory myofibroblastic tumor of the uterus: a clinicopathological, immunohistochemical, and molecular analysis of 13 cases highlighting their broad morphologic spectrum. *Mod Pathol*. 2017;30:1489–1503. doi:10.1038/modpathol.2017.69
24. Collins K, Ramalingam P, Euscher ED, Reques Llanos A, García A, Malpica A. Uterine inflammatory myofibroblastic neoplasms with aggressive behavior, including an epithelioid inflammatory myofibroblastic sarcoma: a clinicopathologic study of 9 cases. *Am J Surg Pathol*. 2022;46:105–117. doi:10.1097/PAS.0000000000001756

International Journal of Women's Health

Dovepress

### Publish your work in this journal

The International Journal of Women's Health is an international, peer-reviewed open-access journal publishing original research, reports, editorials, reviews and commentaries on all aspects of women's healthcare including gynecology, obstetrics, and breast cancer. The manuscript management system is completely online and includes a very quick and fair peer-review system, which is all easy to use. Visit <http://www.dovepress.com/testimonials.php> to read real quotes from published authors.

Submit your manuscript here: <https://www.dovepress.com/international-journal-of-womens-health-journal>